IOSR Journal of Electronics and Communication Engineering (IOSR-JECE)
e-ISSN: 2278-2834,p- ISSN: 2278-8735.Volume 10, Issue 5, Ver. II (Sep - Oct .2015), PP 79-86
www.iosrjournals.org

ANALYSIS OF MULTIPATH FADING PROFILE PROVISION IN MULTIPLE ACCESS SYSTEM GRIDS

Gayatri Mantri[1] , A.Vamsidhar[2]
M.Tech Student, Associate Professor, Head
[1,2]Department of ECE
[1,2]Dadi Institute of Engineering & Technology, Anakapalle

Abstract: *Orthogonal frequency division multiple access (OFDMA) systems exploit multiuser diversity and frequency selectivity to achieve high spectral efficiencies. However, they require considerable feedback for scheduling and rate adaptation, and are sensitive to feedback delays. We develop a comprehensive analysis of the OFDMA system throughput as a function of the feedback scheme, frequency-domain scheduler, and discrete rate adaptation rule in the presence of feedback delays. Previous allocation methods have been iterative nonlinear methods suitable for offline optimization. In the special high sub-channel SNR case, an iterative* radical-jewel *method has linear -time complexity in the number of users and N log N complexity in the number of sub-channels. We propose a non-iterative method that is made possible by our relaxation of strict user rate proportionality constraints. Compared to the* radical-jewel *method, the proposed method waives the restriction of high sub-channel SNR, has significantly lower complexity, and in simulation, yields higher user data rates. Adaptive where, the goal is to redistribute power such that the transmission time of a packet is minimized. While the first two variants decrease transceiver complexity and are simpler, the third is geared towards achieving the maximum throughput possible. We analyze the popular best-n and threshold-based feedback schemes.*
Keywords: *sub channel, OFDMA, feedback, threshold level, sub-carriers*

I. INTRODUCTION

Orthogonal frequency-division multiplexing (OFDM) has recently received increased attention due to its capability of supporting high-data-rate communication in frequency selective fading environments which cause inter-symbol interference (ISI) [1][2]. Instead of using a complicated equalizer as in the conventional single carrier systems, the ISI in OFDM can be eliminated by adding a guard interval which significantly simplifies the receiver structure. However, in order to take advantage of the diversity provided by the multi-path fading, appropriate frequency interleaving and coding is necessary. Therefore, coding becomes an inseparable part in most OFDM applications and a considerable amount of research has focused on optimum encoder, decoder, and interleaver design for information transmission via OFDM over fading environments.

All of the above work is based on the assumption that only the receiver has channel state information (CSI). If information is allowed to flow in the other direction, so that the transmitter and the receiver share all or part of the channel state information, adaptive power and code rate allocation within the OFDM system becomes possible and is expected to achieve significant performance gain. Several adaptive schemes for OFDM systems have been investigated in [2]-[6]. Ditzel [1] proposes an optimal energy allocation scheme among different OFDM sub-carriers which minimizes the total energy necessary to achieve a desired average bit error rate over frequency-selective fading channels. All of the above work is based on the assumption that only the receiver has channel state information (CSI). If information is allowed to flow in the other direction, so that the transmitter and the receiver share all or part of the channel state information, adaptive power and code rate allocation within the OFDM system becomes possible and is expected to achieve significant performance gain. In [2], Czylwik introduces an adaptive modulation scheme for the individual sub-carriers in an OFDM system, and the required signal to noise ratio for certain bit error probabilities is reduced dramatically compared to fixed modulation. Similar adaptive modulation schemes, recommended by Maeda in [3], implement the idea of puncturing codes to delete code bits in non-reliable sub-carriers in an OFDM frame, hence suppressing the total power consumption. Recent research work [4] [5] focuses on joint power, code rate, and modulation allocation among OFDM sub-carriers and achieves comparable performance gains with respect to uniform resource allocation. Piazzo [1] also provides a fast and convergent algorithm on the adaptive power and bit allocation in OFDM systems, which proves to be useful when the channel is changing rapidly.However, most of these approaches focus on uncoded OFDM (or systems with very weak codes) which fails to take advantage of the significant advances that have been made in coding for error correction and detection.

II. Multi User OFDM Systems

In order to adhere to the volatility o f t he wireless medium, combat t he existing interference and ultimately increase achievable data rates, the adoption of sophisticated adaptation techniques is required. When each BS in a cellular network acts independently from other BSs, it is responsible only for users within the coverage area of its cell. The BS is aware of the channel quality of all users and allocates channels to users for down-link transmission [3]. Each channel is allocated to the user that experiences the least interference in it. In that context, transmission parameter adaptation for each user is performed in a straight-forward manner: the BS transmits with sufficient power, so that an acceptable SINR is reached at the receiver, given the measured interference. When the BS employs both power and modulation level adaptation, it can select the highest modulation level for which there exists a power in the range of available transmission power levels, such that a n acceptable SINR is ensured. The BSs ca n take turns in performing the allocation based o n a staggered protocol. The amount of co−channel interference and the susceptibility to it can be controlled by selective insertion of users in a channel and adjustment of transmission parameters. Thus, users can meet their SINR requirements and be maximally “packed” in a channel, so that the total transmission rate in the channel is increased. Furthermore, by appropriate coordination between channel allocation and transmission parameter adaptation, MAC layer QoS of users such as achievable data rates can be more flexibly controlled.

III. Frequency Selective Fading

We have introduced UWB channel path loss and discussed the channel path loss at extended ranges. We now discuss the frequency selective behaviour of the UWB channel. It is however, important to introduce the topic of multipath propagation first. In practice, the beam of radio energy that is sent by the transmitter is not received at the receiver with only one beam, but instead from many beams. These multiple radio beams (after reflection and diffraction on the surface of objects) will arrive at the receiver at a slightly different time and phase. The received rays at the receiver will add up or cancel out which gives rise to multipath fading (rays that have opposite phase will add up destructively).

Multipath fading is also referred to as frequency selective fading. This frequency selective fading distorts the received signal when the frequency components of the signal are not all affected equally [8]. More specifically, frequency selective fading

happens when the signal’s spectrum is wider than the channel coherence bandwidth, and hence the spectrum components that are outside the coherence bandwidth will be affected differently than those within the coherence bandwidth. An illustration is shown where in Figure ,

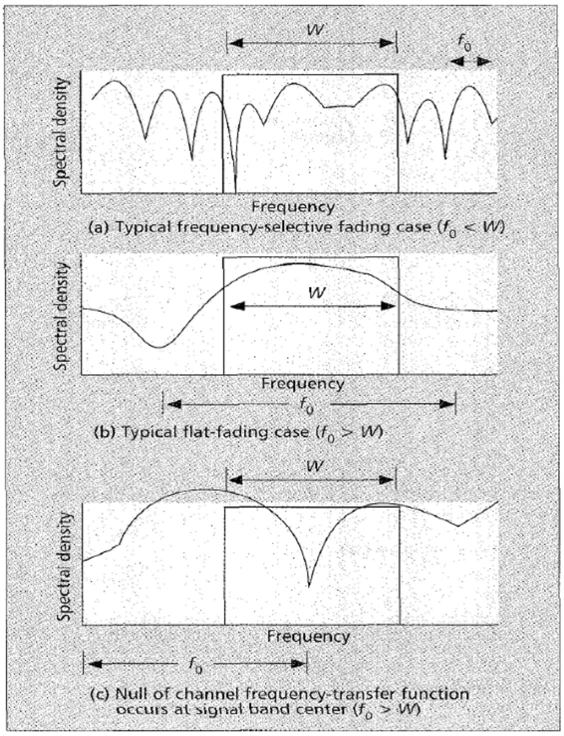

where f0 is the coherence bandwidth.

IV. Relationships between the channel frequency-transfer function

UWB Channel Coherence Bandwidth

The channel coherence bandwidth can be expressed in the following equation, which shows that the coherence bandwidth is inversely proportional to the factor Δ, where Δ is the delay spread.

In this particular channel impulse response, the root mean square delay spread is 15ns [4], which in turn provides us with an indirect measure of a UWB channel coherence bandwidth. The relationship between coherence bandwidth and the channel delay spread has been specified in [8]. A coherence bandwidth that is equal to the inverse of the RMS delay spread means that frequencies that are located close to each other within the coherence bandwidth can be considered as experiencing the same fading. In [4], the author claims that a higher delay spread of 25 ns can cover worst case situations. In this case the inverse of the delay spread is 40MHz. Hence, the spectrum components that lie within 40MHz will experience the same fading. It is now obvious that frequency selective fading is unavoidable as the UWB transmission uses a minimum of 512MHz bandwidth. On the other hand, the assumption that we made later in our simulation that subcarriers of 4.125MHz will have the same amount of fading within that bandwidth is reasonable.

In any radio transmission, the channel spectral response is not flat. It has dips or fades in the response due to reflections causing cancellation of certain frequencies at the receiver. Reflections off near-by objects (e.g. ground, buildings, trees, etc) can lead to multipath signals of similar signal power as the direct signal. This can result in deep nulls in the received signal power due to destructive interference. For narrow bandwidth transmissions if the null in the frequency response occurs at the transmission frequency then the entire signal can be lost. This can be partly overcome in two ways. By transmitting a wide bandwidth signal or spread spectrum as CDMA, any dips in the spectrum only result in a small loss of signal power, rather than a complete loss. Another method is to split the transmission up into many small bandwidth carriers, as is done in a COFDM/OFDM transmission. The original signal is spread over a wide bandwidth thus, any nulls in the spectrum are unlikely to occur at all of the carrier frequencies. This will result in only some of the carriers being lost, rather then the entire signal. The information in the lost carriers can be recovered provided enough forward error corrections is sent.

The presence of reflectors in the environment surrounding a transmitter and receiver create multiple paths that a transmitted signal can traverse. As a result, the receiver sees the superposition of multiple copies of the transmitted signal, each traversing a different path. Each signal copy will experience differences in attenuation, delay and phase shift while travelling from the source to the receiver. This can result in either constructive or destructive interference, amplifying or attenuating the signal power seen at the receiver. Strong destructive interference is frequently referred to as a deep fade and may result in temporary failure of communication due to a severe drop in the channel signal-to-noise ratio.

V. SYSTEM MODEL

In order to understand the mathematical principles of OFDM systems, let us first take an overview of the time domain uncoded OFDM system model, which is shown in Fig. 1.

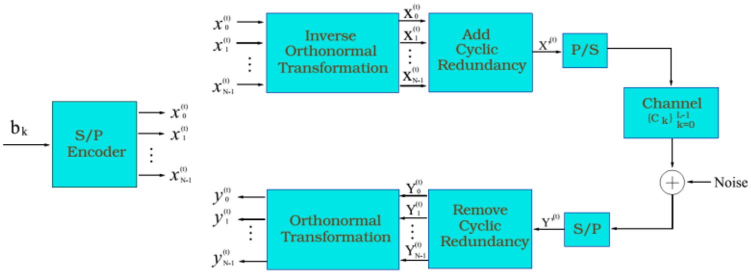

Fig 1 Time domain OFDM system model

Let bk represent the binary data sequence to be transmitted over the channel. This data is divided into non-overlapping blocks of n = N · log2 M bits. The n bits of data are partitioned into N groups, with each log2 M bits mapped into a complex symbol of constellation size M. Symbol x(kt) is the signal transmitted over the kth subcarrier during the t-th OFDM frame. At the transmitter, an inverse discrete Fourier transform (IDFT) is performed as a method of modulation, which results in samples Xk(t) given by

$$X_k^{(t)} = \frac{1}{\sqrt{N}} \sum_{i=0}^{N-1} x_i^{(t)} \cdot \exp(j\frac{2\pi ki}{N}), \quad 0 \leq i \leq N-1$$

Assume that the channel is frequency-selective, and hence the implementation of a cyclic redundancy of sufficient length to the N-point OFDM frame is an effective method to counter inter symbol interference (ISI) caused by the channel. The cyclic prefix causes the sequence {Xk(t) } to appear periodic to the channel and clears the channel memory at the end of each OFDM frame. This action makes successive transmissions independent. The output from the channel, with additive noise Nk(t), may be written as

$$Y_k^{(t)} = c_k^{(t)} \star X_k(t) + N_k^{(t)}$$

Equivalent Frequency Domain Coded OFDM System Model

Although the time domain model provided in the previous section is conceptually straightforward, it is much more insightful to analyze the OFDM system in the frequency domain since the information symbols modulate different subcarriers in the frequency domain. Hence, let us consider the frequency model for a coded OFDM system illustrated in Fig. 2. A block of k information bits, denoted as b = (b1, · · · , bk), is encoded into a codeword x = (x1, · · · , xn) of length n, where each symbol xi is an element from a complex alphabet X. There are a total of m codewords in the code book and the code rate is defined to be R = (log2 m)/n. Note that here we combine encoder, modulator, and interleaver together to form one super encoder E.

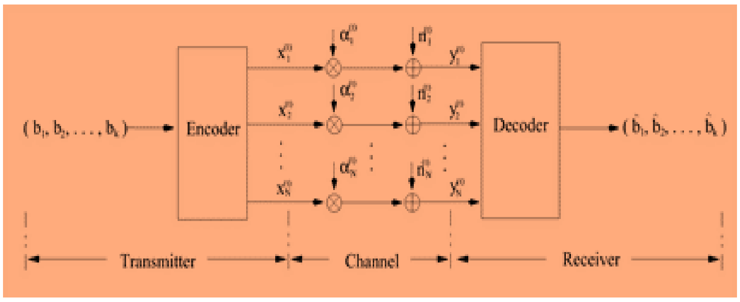

Fig 2 Frequency domain OFDM system model

The individual frame is transmitted by N dependent parallel subchannels, each representing a different OFDM sub-carrier. According to the tapped delay-line model [7], the fading coefficients αi(t) of the tth OFDM frame are related to the fading envelopes c(it) through

The Concept of Instantaneous Channel Capacity

The well known Shannon capacity theory states that we can send information with arbitrarily low error probability as long as the rate in bits per channel use is less than the channel capacity [18]. But this capacity is achieved upon coding over time with an infinite or huge codeword length. In coded OFDM systems, coding is performed in the frequency domain instead of the time domain, where only a limited number of OFDM frames are taken to form one codeword. Thus the maximum achievable information rate or the channel capacity of a coded OFDM system and its relationship with the conventional channel capacity of an AWGN channel presents an interesting research problem.

By combining the OFDM symbols in the same sub-carrier position over a sufficient large number of OFDM frames to form one code word, an infinite or huge decoding delay is introduced, which is intolerable in some applications. In coded OFDM, the only difference is that coding is performed in the frequency domain over a sufficiently large number of sub-carriers N, instead of coding in the time domain over a larger number of time slots and combining these n sub-channels together. In doing so, only a limited amount of decoding delay is introduced, which is tolerable in most applications. The more important issue is that we do not have to apply different alphabets or information rates for each sub-carrier due to differing signal to noise ratios. Thus it is meaningful to study the behaviour of this instantaneous channel capacity.

First, instead of having independent fading on different sub-channels in a block fading channel, the fading coefficients αi(t) of different OFDM sub-carriers are correlated. Second, even though each OFDM sub-carrier has block length 1 when viewed as a parallel block fading channel, the convergence of the upper bound and lower bound still exists for OFDM system having large number of subcarriers as is shown in the following section. This is in contrast to the convergence condition of a block fading channel (large block length).

VI. Performance Analysis Of Coded OFDM Systems

Based on the information theoretical analysis in the previous chapter, analytical system performance analysis is provided in this section. Here we assume each codeword is composed of only one OFDM frame (l = 1), and omit the superscript t in vectors x(t), y(t), c(t), and α(t). Extending the analysis to coded OFDM systems whose coding is performed on more than one OFDM frames is straightforward.

Theoretically, the outage probability is greater than the lower bound but less than the upper bound which is exactly the case shown in the above plot, although only an approximated result is used here. Further from Fig. 4, we see that the lower bound is only about 1dB from the upper bound, which indicates that both of these bounds and also the approximated outage probability are quite tight and a valid performance indication of the system for large block lengths.

VII. OFDM Parameters

Table 1 lists the main parameters of the draft OFDM standard. A key parameter which largely affected the choice of the other parameters is the guard interval of 800 ns. This guard interval provides robustness to root-mean-squared delay spreads up to several hundreds of nanoseconds, depending on the coding rate and modulation used. In practice, this means that the modulation is robust enough to be used in any indoor environment, including large factory buildings. It can also be used in outdoor environments, although directional antennas may be needed in this case to reduce the delay spread to an acceptable amount and to increase the range.

Table 1: Main Parameters of the OFDM standard.

Data rate	6, 9, 12, 18, 24, 36, 48, 54 Mbit/s
Modulation	BPSK, QPSK, 16-QAM, 64-QAM
Coding rate	1/2, 2/3, ¾
Number of subcarriers	52
Number of pilots	4
OFDM symbol duration	4 µs
Guard interval	800 ns
Subcarrier spacing	312.5 kHz
-3 dB Bandwidth	16.56 MHz
Channel spacing	20 MHz

In order to limit the relative amount of power and time spent on the guard time to 1 dB, the symbol duration was chosen to be 4 µs. This also determined the subcarrier spacing to be 312.5 kHz, which is the inverse of the symbol duration minus the guard time. By using 48 data subcarriers, uncoded data rates of 12 to 72 Mbps can be achieved by using variable modulation types from BPSK to 64-QAM. In order to correct for subcarriers in deep fades, forward error correction across the subcarriers is used with variable coding rates, giving coded data rates from 6 up to 54 Mbps. Convolutional coding is used with the industry standard rate 1/2, constraint length 7 code with generator polynomials. Higher coding rates of 2/3 and 3/4 are obtained by puncturing the rate 1/2 code.

VIII. Channelization

Figure 1 shows the channelization for the lower and middle Unlicensed National Information Infra-structure (UNII) bands. Eight channels are available with a channel spacing of 20 MHz and guard spacings of 30 MHz at the band edges in order to meet the stringent FCC restricted band spectral density requirements. The FCC also defined an upper UNII band from 5.725 to 5.825 GHz, which carries another 4 OFDM channels. For this upper band, the guard spacing from the band edges is only 20 MHz, since the out-of-band spectral requirements for the upper band are less severe as those of the lower and middle UNII bands. Notice that different carrier frequencies may be used in Europe and Japan, but the channel spacing will be the same, while also most of the bands are expected to overlap.

IX. OFDM Signal Processing

A general block diagram of an OFDM transceiver is shown in figure 2. In the transmitter path, binary input data is encoded by a rate 1/2 convolutional encoder. The rate may be increased to 2/3 or 3/4 by pucturing the coded output bits. After interleaving, the binary values are converted into QAM values. To facilitate coherent reception, 4 pilot values are added to each 48 data values, so a total of 52 QAM values is reached per OFDM symbol, which are modulated onto 52 subcarriers by applying the Inverse Fast Fourier Transform (IFFT). To make the system robust to multipath propagation, a cyclic prefix is added. Further, windowing is applied to get a narrower output spectrum. After this step, the digital output signals can be converted to analog signals, which are then upconverted to the 5 GHz band, amplified and transmitted through an antenna.

The OFDM receiver basically performs the reverse operations of the transmitter, together with additional training tasks. First, the receiver has to estimate frequency offset and symbol timing, using special training symbols in the preamble. Then, it can do a Fast Fourier Transform for every symbol to recover the 52 QAM values of all subcarriers. The training symbols and pilot subcarriers are used to correct for the channel response as well as remaining phase drift. The QAM values are then demapped into binary values, after which a Viterbi decoder can decode the information bits.

X. OUTPUTS

The comparison of total capacities between the proposed method LINEAR and ROOT -FINDING. Notice that the capacities increase as the number of users increases. This is the effect of multiuser diversity gain, which is more prominent in systems with larger number of users. The previously proposed method has a consistently higher total capacity than the Radical-Jewel method for all the numbers of users

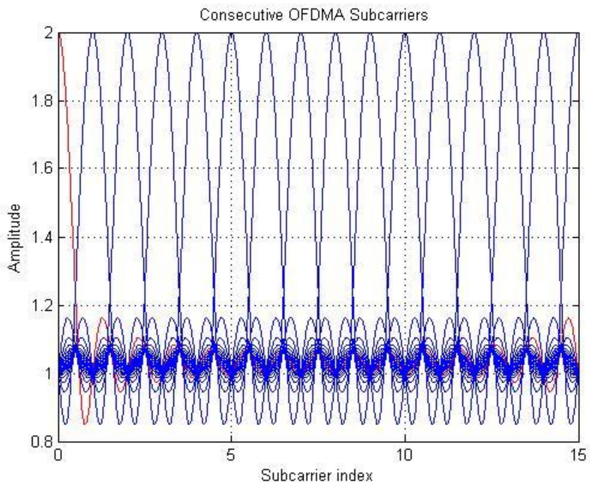

Fig 3 OFDMA Subcarriers

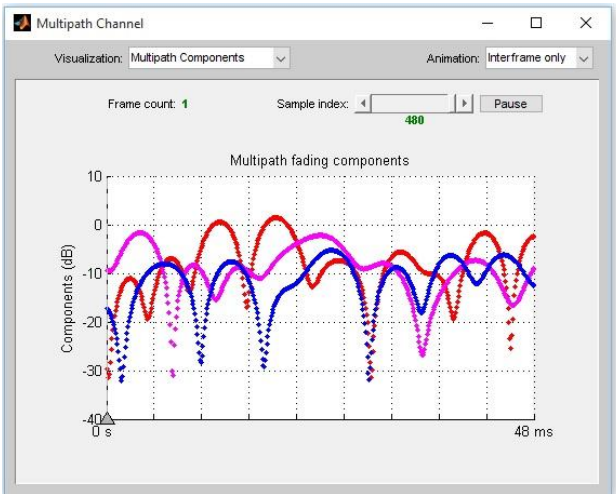

Fig 4 OFDMA Subcarriers

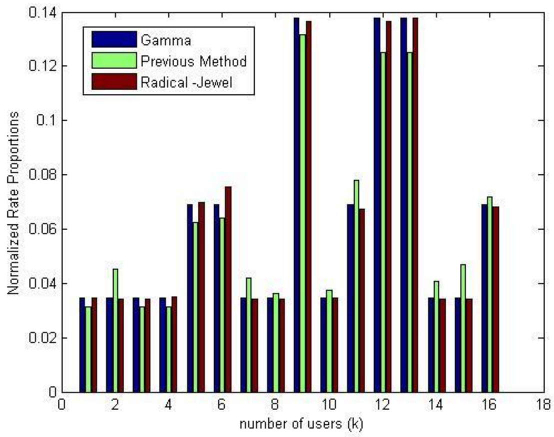

Fig 5 OFDMA Subcarriers

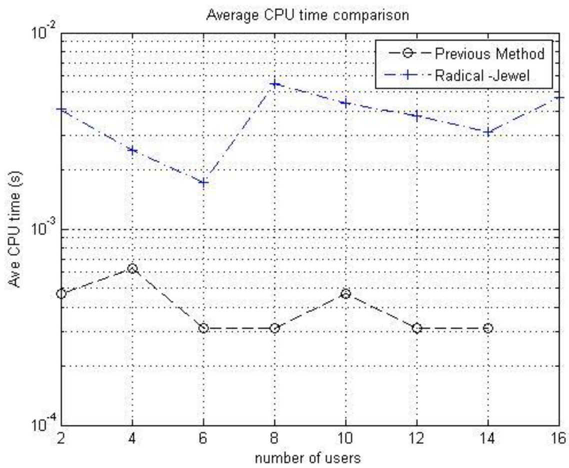

Fig 6 OFDMA Subcarriers

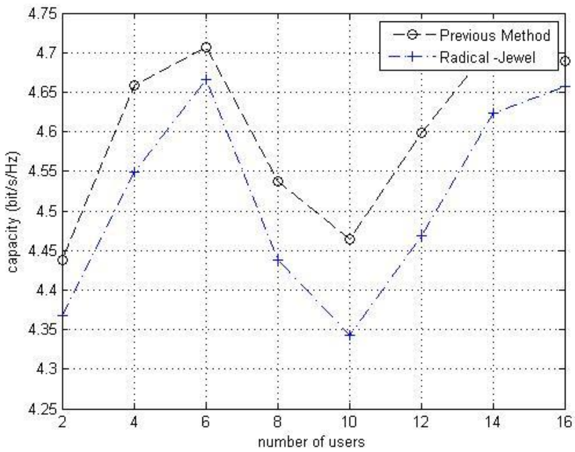

Fig 7 OFDMA Subcarriers

XI. CONCLUSION

A game based approach has been investigated and implemented to solve the short range DCPA problem where the interference from homogeneous devices deployed in the close vicinity is the major concern; and a longer range DCPA problem where the channel path loss over longer ranges is the major concern. This is significantly more complex than the simple operations required in the Previous Proposed power allocation method, especially when considering implementation in fixed point arithmetic. Furthermore, the Radical -Jewel power allocation method also needs a high sub-channel SNR assumption to function properly, which the

Previous proposed method does not make. This work presents a new method to solve the rate-adaptive resource allocation problem with proportional rate constraints for OFDMA systems. It improves on the earlier work by developing a novel subcarrier allocation scheme that achieves approximate rate proportionality while maximizing the total capacity. This scheme was also able to exploit the special linear case, thus allowing the optimal power allocation to be performed using a direct algorithm with a much lower complexity versus an iterative algorithm. It is shown done simulation that the proposed method performs better than the previous work in terms of significantly decreasing the computational complexity, and yet achieving higher total capacities, while being applicable to a more general class of systems.

REFERENCES

[1]. P. Y. Glorennec, "Fuzzy Q-learning and dynamical fuzzy Q-learning," in Fuzzy Systems, 1994. IEEE World Congress on Computational Intelligence., Proceedings of the Third IEEE Conference, 1994, pp. 474-479 vol.1.

[2]. Y. Nagayuki, S. Ishii, and K. Doya, "Multi-agent reinforcement learning: an approach based on the other agent's internal model," in MultiAgent Systems, 2000. Proceedings. Fourth International Conference, 2000, pp. 215-221.

[3]. D. Manstretta, N. Laurenti, and R. Castello, "A Reconfigurable Narrow-Band MBOFDM UWB Receiver Architecture," Circuits and Systems II: Express Briefs, IEEE Transactions, vol. 55, pp. 324-328, 2008.

[4]. V. Shah, N. B. Mandayam, and D. J. Goodman, "Power Control for Wireless Data Based on Utility and Pricing," in Personal, Indoor and Mobile RadioCommunications, 1998. The Ninth IEEE International Symposium on, 1998, pp. 1427- 1432 vol.3.

[5]. H. Wymeersch, S. Marano, W. M. Gifford, and M. Z. Win, "A Machine Learning Approach to Ranging Error Mitigation for UWB Localization,"Communications, IEEE Transactions, vol. 60, pp. 1719-1728, 2012.

[6]. E. Driouch, W. Ajib, and A. Ben Dhaou, "A greedy spectrum sharing algorithm for cognitive radio networks," in Computing, Networking and Communications (ICNC), 2012 International Conference, 2012, pp. 1010-1014.

[7]. D. H. Niyato, "Competitive spectrum sharing in cognitive radio networks: a dynamic game approach," Wireless Communications, IEEE Transactions, vol. 7, pp. 2651 - 2660, July 2008 2008.

[8]. D. Cabric, S. M. Mishra, and R. W. Brodersen, "Implementation issues in spectrum sensing for cognitive radios," in Signals, Systems and Computers, 2004. Conference Record of the Thirty-Eighth Asilomar Conference, 2004, pp. 772-776 Vol.1.